Compression of femtosecond laser pulses in thin one-dimensional photonic crystals

A. V. Andreev, A. V. Balakin, I. A. Ozheredov, and A. P. Shkurinov
Department of Physics and International Laser Center, M. V. Lomonosov Moscow State University, Moscow 119899, Russia

P. Masselin, G. Mouret, and D. Boucher
Laboratoire de PhysicoChimie de l' Atmosphère, CNRS EP 1831, Université du Littoral, 145 avenue Maurice Schumann, 59140 Dunkerque, France

(Received 17 May 2000; published 19 December 2000)

We demonstrate experimentally the effect of compression of femtosecond laser pulses in thin (a few micrometers) one-dimensional photonic crystal. We show that the compression effect is reasonably described by the linear dispersion properties of the photonic crystal itself and the quadratic dispersion approximation cannot be efficiently used for the description of interaction of the femtosecond laser pulses with the thin photonic crystal. For given parameters of the femtosecond pulse it leads to the existence of the optimal dimension of the photonic crystal from the point of view of the compression efficiency. Due to the wide spectral width of the femtosecond laser pulses the high-order dispersion effects play an important role in pulse propagation in photonic crystals and as a result the pulse compression occurs for both positive and negative signs of chirp of the incoming femtosecond pulses.

DOI: 10.1103/PhysRevE.63.016602 PACS number(s): 42.70.Qs, 42.65.Re, 68.65.−k

I. INTRODUCTION

Since the earlier development of the dynamic theory of x-ray diffraction by Sir Lawrence Bragg [1] and much earlier antecedents that one may already find in [2], the studies of photonic band gap (PBG) materials [3] have been a real challenge for scientists. However, only during the last six years we have observed the avalanchelike growth of the number of publications on the studies of optical phenomena in PBG materials. The motivation for research of photonic crystals (PC) [3,4] that are the artificial multidimensional structures with the periodic modulation of one of the dielectric functions [5] is due to their fundamental property to have the PBG where the propagation of light in the case of linear interaction is forbidden [6]. The problem of the studies of the PBG properties in three-dimensional crystals is rather complicated, as it needs computational solution of Maxwell's vectorial equations in the nonuniform dielectric medium [7]. In many cases the three-dimensional problem may be reduced to the analytically soluble one-dimensional one [8,9]. A structure with the periodic modulation of the refraction index and/or nonlinear optical susceptibility with the period closer to the wavelength of light may be accepted as a model of one-dimensional PC. Such crystals can also be characterized by the presence of PBG with the total Bragg reflection regime for the optical radiation.

A specific case for the research of PC is the study of interaction of the light pulses and, in particular, the ultrashort pulses with the PC structures. In this case one should take into account that the pulse regime has several advantages and specific properties [10]. The most obvious one is that high power that is needed for the investigation of nonlinear optical processes is more easily achieved with the ultrashort pulses, and the application of these pulses makes possible its study without sample destruction. In [11] the parametric amplification of picosecond pulses in the Bragg grating is investigated. In our recent experiments [12–14] with the femtosecond laser pulses we demonstrated that near the PBG edge the specific enhancement of the nonlinear optical phenomena such as second-harmonic and sum-frequency generation may take place.

The first observation of the nonlinear propagation effects in optical fibers with the Bragg grating was demonstrated by B. Eggleton in [15,16]. Later in [17,18] the authors studied the effect of picosecond laser pulses compression and ''solitonlike'' propagation due to the simultaneous effect of self-phase modulation associated with the Kerr effect and the large dispersion in the Bragg grating induced in the optical fibers. The effects of this type were theoretically described by H.G. Winful in [19] for nonlinear compression in weakly modulated optical fibers and later by the authors of [20,21] for the submillimeter one-dimensional PC with the relatively deep modulation of the refraction index.

Propagation of the ultrashort light pulses through the PC depends not only on the dispersion properties of the PC near the PBG area, but also on the intensity of the field inside the structure [15]. This ''dynamic compression'' is caused by the perturbation of the refraction index due to the nonlinear interaction of the incoming pulse with the PC periodic media. This ''dynamic'' effect takes place in the case of localization of the field of the pulse inside the layers that have high refraction index and/or the nonlinearity [22] and has particular interest for the description of the nonlinear compression in the photonic structures with the large modulation of the refraction index [23].

The subject of this paper is the study of compression of the femtosecond laser pulses in thin one-dimensional PC that is prepared in the form of multilayer structure with the modulation of refraction index. In the experiments we used the laser pulses of femtosecond duration and PC with the deep modulation of the refraction index ($\Delta n = 0.8$). Until now the experiments on the compression of the ultrashort pulses were performed in the picosecond time scale and the problem of compression of femtosecond laser pulses in PC

was not experimentally studied. Moreover, the experiments were mainly performed with the optical Bragg grating models of PC or with the PC of submillimeter thickness. In our initial experimental observation of the compression in the thin one-dimensional PC [24], the agreement between the experiment and the numerical calculation was qualitative. In contrast, in the present paper we describe experimental results that already agree quantitatively with the theory. It should be noted that the presented experimental results could be explained without application of the mechanisms of nonlinear compression [15,17–20,23]. To our knowledge, the detailed studies of mechanisms of linear compression, in particular for femtosecond laser pulses, are not presented in the literature yet, though some successful attempts are known [25,26]. It makes such studies and the presented results interesting from a fundamental physics point of view, and could have important applications in technology.

II. PREPARATION OF ONE-DIMENSIONAL PHOTONIC CRYSTAL

In this paper we consider a one-dimensional PC structure consisting of ZnS and SrF_2 layers deposited on a glass substrate. It is composed of 15 layers: eight alternate layers of high (ZnS, $n_1=2.29$) and seven of low (SrF_2, $n_2=1.46$) refraction index ones [12].

The layers have thickness $d_i=3\lambda/4n_i$ $(i=1,2)$ for the reference wavelength $\lambda_0=790$ nm to form the quarter-wave stack for the wavelength λ_0. The total thickness of PC sample is roughly equal to $L=4.8$ μm for the reference wavelength λ_0. This PC structure strongly reflects light at the normal incidence in the wavelength range of 745–830 nm.

In the theoretical part of the paper all the simulations are made taking into account the parameters of the described above structure and 550 fs pulse duration at the wavelength 812 nm. The pulse is frequency modulated with spectral width of $\Delta\omega/\omega_0=10^{-2}$.

III. THEORY

A. Wave equation

The propagation of electromagnetic wave in the one-dimensional periodic medium is described by the wave equation:

$$\Delta\vec{E}-\frac{\epsilon(z)}{c^2}\frac{\partial^2\vec{E}}{\partial t^2}=0, \tag{1}$$

where the dielectric permittivity $\epsilon(z)$ is a periodic function of the coordinate z. When we deal with the process of the wave propagation in the linear periodic medium it is convenient to expand the field in Fourier integral

$$\vec{E}(\vec{r},t)=\int d\vec{k}\int d\omega\vec{E}(\vec{k},\omega,z)\cdot\exp[i(\vec{k}\cdot\vec{\rho}-\omega t)],$$

where $\vec{\rho}\{x,y,0\}$ is a two-dimensional radius-vector in the entrance plane of the PC structure. By substituting this expansion into Eq. (1) we get

$$\frac{d^2\vec{E}}{dz^2}+\kappa^2(\chi(z)+\cos^2\theta)\vec{E}=0, \tag{2}$$

where $\kappa=2\pi c/\lambda$, λ is the wavelength, θ is the incidence angle, $\chi=\epsilon-1$ is the dielectric susceptibility multiplied by 4π. There is a number of different methods of analyzing and solving of equation Eq. (2).

B. Recurrence relationships

One of the effective methods of the study of the optical properties of periodic media is based on the using of recurrence procedure [27]. The reflection and transmission coefficients of a one-dimensional periodic structure consisting of the bilayers of materials with the dielectric permittivity $\epsilon_{1,2}$ and thickness $d_{1,2}$ can be determined by the following recurrence relationships:

$$R_n=R_{n-1}+\frac{R_1\overline{T}_{n-1}T_{n-1}}{1-R_1\overline{R}_{n-1}}, \tag{3a}$$

$$\overline{R}_n=\overline{R}_1+\frac{\overline{R}_{n-1}\overline{T}_1T_1}{1-R_1\overline{R}_{n-1}}, \tag{3b}$$

$$T_n=\frac{T_1T_{n-1}}{1-R_1\overline{R}_{n-1}}, \tag{3c}$$

$$\overline{T}_n=\frac{\overline{T}_1\overline{T}_{n-1}}{1-R_1\overline{R}_{n-1}}, \tag{3d}$$

where the reflection and transmission coefficients for a structure consisting of N periods are denoted by R_n and T_n for the case of incidence on the structure from the side of high refraction index material and $\overline{R}_n$ and $\overline{T}_n$ for the opposite case. Recurrence relationships (3) also enable us to express the optical parameters of one period of structure in terms of the optical parameters of its constituent layers. For example

$$R_1=r_1+\frac{r_2t_1^2}{1-\overline{r}_1r_2}, \tag{4a}$$

$$T_1=\frac{t_1t_2}{1-\overline{r}_1r_2}, \tag{4b}$$

where

$$r_i=\frac{r_F^{(i)}(1-\exp(i2\phi_i))}{1-(r_F^{(i)})^2\exp(i2\phi_i)},$$

$$t_i=\frac{t_F^{(i)}\overline{t}_F^{(i)}\exp(i\phi_i)}{1-(r_F^{(i)})^2\exp(i2\phi_i)},$$

where $\phi_i=k_z^{(i)}d_i$. In the last equation $r_F^{(i)}$ and $t_F^{(i)}$ are the Fresnel reflection and transmission coefficients. In the case of s-polarized incident wave they are expressed in terms of

the normal projections of the wave vectors in vacuum $\kappa_z = \kappa \cos\theta$ and in medium $k_z^{(i)} = \kappa\sqrt{\cos^2\theta + \chi_i}$ in the following way:

$$r_F^{(i)} = \frac{\kappa_z - k_z^{(i)}}{\kappa_z + k_z^{(i)}}, \tag{5a}$$

$$t_F^{(i)} = \frac{2\kappa_z}{\kappa_z + k_z^{(i)}}, \tag{5b}$$

$$\overline{t_F^{(i)}} = \frac{2k_z^{(i)}}{\kappa_z + k_z^{(i)}}. \tag{5c}$$

In the analyses of the wave propagation in transparent periodic media it is useful to keep in mind the following relationships between the reflection and transmission coefficients.

$$T_n = \overline{T_n}, \tag{6a}$$

$$R_n = R\sqrt{\frac{R_1}{\overline{R_1}}}, \tag{6b}$$

$$\overline{R_n} = R\sqrt{\frac{\overline{R_1}}{R_1}}. \tag{6c}$$

Thus, in the transparent (nonabsorbing) medium the reflection coefficients can be represented in the form $R_n = R\exp(i\phi_R)$, $\overline{R_n} = R\exp(-i\phi_R)$, and in this case the phase of transmission coefficient ϕ_T differs from ϕ_R by $\pm\pi/2$.

The solution of Eq. (2) can be represented in the following form:

$$E(z) = u(z)\exp(iqz), \tag{7}$$

where $u(z)$ is a periodic function, and q is a quasimomentum or Bloch wave vector. If we apply the recurrence procedure to the semi-infinite medium we can easily get the following equations for the semi-infinite periodic medium reflection coefficient R and Bloch wave vector q:

$$R^2 - \frac{1 + R_1\overline{R_1} - T_1^2}{\overline{R_1}}R + \frac{R_1}{\overline{R_1}} = 0, \tag{8}$$

$$\exp(i2qd) - \frac{1 - R_1\overline{R_1} + T_1^2}{T_1}\exp(iqd) + 1 = 0, \tag{9}$$

where $d = d_1 + d_2$ is the period of structure. If the top layer of structure is low refraction index layer then the reflection coefficient is $\overline{R} = R\overline{R_1}/R_1$.

C. Quasi-momentum

Quasi-momentum q determines the dispersion properties of semi-infinite periodic medium. One of the solutions of the quadratic equation Eq. (9) corresponds to the wave exponentially decreasing with depth. For this wave we have $\mathrm{Im}(q) > 0$. In the semi-infinite medium we should omit the second solution with $\mathrm{Im}(q) < 0$, because it corresponds to the wave exponentially increasing with depth and is not a physical solution.

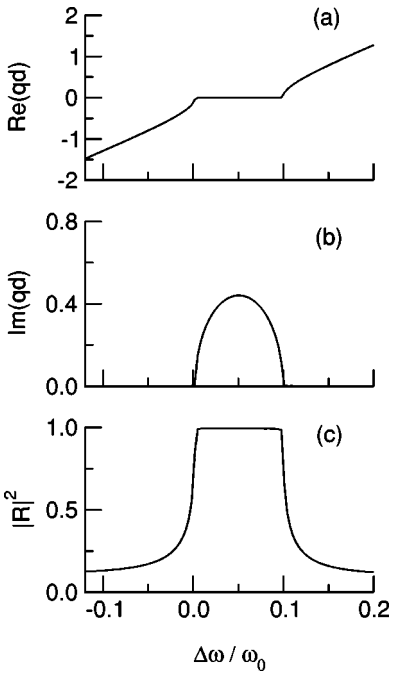

FIG. 1. Real (a), imaginary (b) parts of the quasimomentum and the energy reflection coefficient $|R|^2$ (c) as a function of the scaled frequency detuning $\Delta\omega/\omega_0$. The pulse carrier frequency $\omega_0 = 2\pi c/\lambda_0$ corresponds to the wavelength $\lambda_0 = 812$ nm.

In Fig. 1 for the case of normal incidence we plot the real (a) and imaginary (b) parts of the quasi-momentum and in Fig. 1(c)—the energy reflection coefficient $|R|^2$ as a function of the scaled frequency detuning $\Delta\omega/\omega_0$, where the pulse carrier frequency $\omega_0 = 2\pi c/\lambda_0$ corresponds to the wavelength $\lambda_0 = 812$ nm. The relative detuning varies in the interval $-0.12 \leqslant \Delta\omega/\omega_0 \leqslant 0.2$. In the region far from photonic band gap we can clearly see the linear dependency between the real part of quasimomentum and frequency. In contrast there is a high dispersion in the region near the photonic band gap and at its edges. The imaginary part of quasimomentum differs from zero only in the photonic band gap. Thus the frequency dispersion effects are most pronounced in the region near the photonic band gap.

Figure 2(a) shows the real part of quasimomentum as a function of incidence angle at a given frequency corresponding to the wavelength $\lambda_0 = 812$ nm. The angular dependency of the energy reflection coefficient $|R|^2$ is shown in Fig. 2(c). For comparison, the dotted line in Fig. 2(a) shows the angular dependency of the phase $k_z d = k_z^{(1)} d_1 + k_z^{(2)} d_2$ that transmitted wave could have in the absence of dispersion. We can see that in the region far from the photonic band gap $q \approx k_z$. Figure 2(b) shows the real part of the difference $(q - k_z)d$ as a function of the angle of incidence. It is definitely seen that there are at least three different angular in-

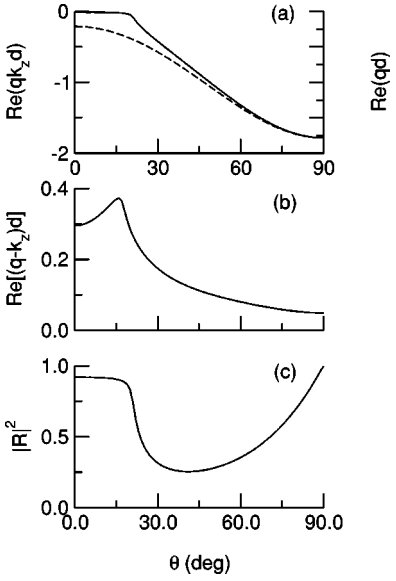

FIG. 2. (a) Real part of quasimomentum as a function of incident angle at given frequency corresponding to the wavelength $\lambda_0 = 812$ nm (solid line) and angular dependency of the phase $k_z d = k_z^{(1)} d_1 + k_z^{(2)} d_2$ that transmitted wave could have in the absence of the dispersion (dotted line); (b) Difference $(q - k_z)d$ versus angle of incidence; (c) Angular dependency of the energy reflection coefficient $|R|^2$.

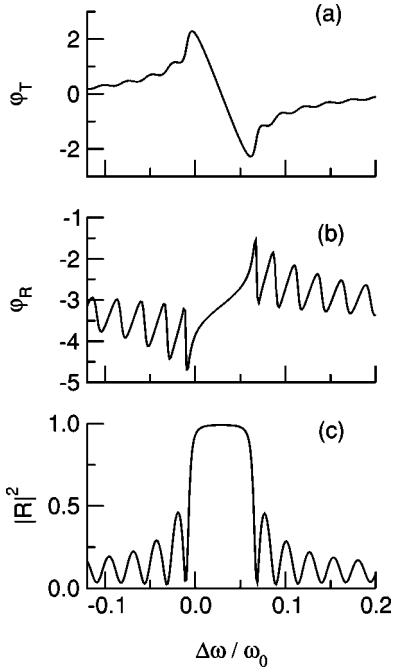

FIG. 3. Phases of the transmitted into the substrate (a) and reflected (b) waves and energy reflection coefficient $|R|^2$ (c) as a function of the scaled frequency detuning $\Delta\omega/\omega_0$.

tervals where quasimomentum $q(\theta)$ can be approximated by the parabolic function.

$$q(\theta) = q(\theta_0) + q'(\theta_0)(\theta - \theta_0) + q''(\theta_0)\frac{(\theta - \theta_0)^2}{2}.$$

The first and second derivatives $q'(\theta_0)$ and $q''(\theta_0)$ are different in different angular intervals. The second derivative $q''(\theta_0)$ has the highest value at the edge of the photonic band gap, $\theta_0 = \theta_{PBG}$, and it is negative here.

Hence, similar to the frequency dispersion effects, the spatial dispersion effects are most pronounced in the region near the photonic band gap.

D. Structure of finite length

In the previous section we have shown that the strong frequency and spatial dispersion near and at the edge of the photonic band gap is the most prominent feature of the dispersion properties of the semi-infinite structures. It is evident that these properties are inherited by the periodical structure with a finite number of spatial periods. In this section we discuss the specific features of dispersion properties of the finite length structures.

We have mentioned in the previous section that one of the solutions of Eq. (9) for quasimomentum is a nonphysical solution in semi-infinite medium. In the medium of the finite length both solutions are physical and the second one corresponds to the wave reflected at the bottom of the structure and propagating towards its top layer. The presence of two counter-propagating waves will result in the appearance of oscillations in dispersion dependencies due to interference phenomena.

Figure 3 shows the phases of the transmitted into the substrate (a) and reflected (b) waves and energy reflection coefficient $|R_n|^2$ (c) as a function of frequency detuning in the same interval as in Fig. 1. This figure is for the normal incidence case. For convenience what we really show in Fig. 3(a) is the difference:

$$\phi_T - (8k_z^{(1)}d_1 + 7k_z^{(2)}d_2).$$

It should be reminded that the structure under consideration consists of eight layers of ZnS and seven layers of SrF_2 deposited on glass substrate. We can see the strong frequency dispersion at the edge of photonic band gap and oscillations near it. These oscillations are most pronounced in the phase of the reflected wave. We can also see that taking into account substrate and absorption occurring in real medium breaks the relationship, mentioned in Sec. III B, between the phases of transmitted and reflected waves.

Figure 4 shows the phases of the transmitted (a) and reflected (b) waves and energy reflection coefficient (c) versus the angle of incidence for the same λ_0. Figure 5 shows the reflection coefficient $|R|^2$ of the ZnS/SrF_2 PC structure under study measured on the wavelength 814 nm with the *s*-incoming and *s*-analyzing polarizations of light for various angles of incidence. By the dashed line we show the copy of Fig. 4(c) for comparison. On Figs. 4 and 5 one can see again the strong oscillations due to the interference of the counter-propagating waves. The experimental data show good agreement with the presented above model.

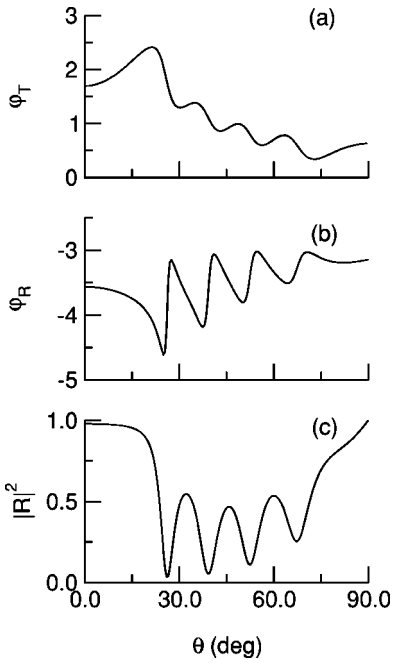

FIG. 4. Phases of the transmitted (a) and reflected (b) waves and energy reflection coefficient (c) as function of incident angle.

E. Pulse compression

Equations (1) and (2) produce the following equations for the field amplitude of the transmitted and reflected waves:

$$E_T(\vec{\rho},z=L,t)=\int\int E(\vec{k},\omega,z=0)\cdot T_n(\vec{k},\omega)\cdot\exp[i(\vec{k}\cdot\vec{\rho}-\omega t)]\mathrm{d}\vec{k}\mathrm{d}\omega, \tag{10}$$

$$E_R(\vec{\rho},z=0,t)=\int\int E(\vec{k},\omega,z=0)\cdot R_n(\vec{k},\omega)\cdot\exp[i(\vec{k}\cdot\vec{\rho}-\omega t)]\mathrm{d}\vec{k}\mathrm{d}\omega, \tag{11}$$

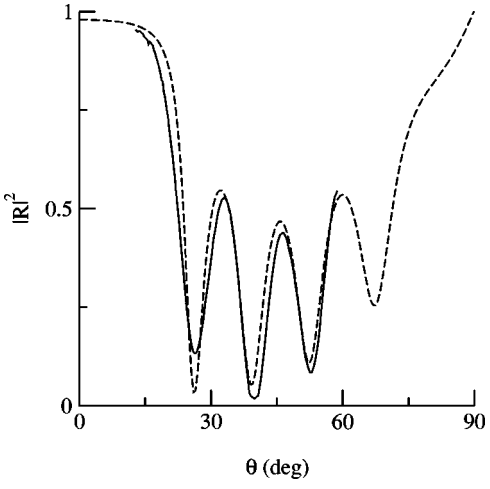

FIG. 5. Reflection coefficient $|R|^2$ of the ZnS/SrF_2 PC structure under study versus the angle of incidence measured on the wavelength $\lambda=814$ nm with the *s*-incoming and *s*-analyzing polarizations of the light. By the dashed line we show comparative the copy of Fig. 4(c).

where L is thickness of PC. The amplitude of incident chirped pulse is

$$E(\vec{\rho},z=0,t)=E_0(\vec{\rho})\cdot\exp\left[i(\vec{k}_0\cdot\vec{\rho}-\omega_0 t)-\frac{1}{2}\left(\frac{t^2}{\tau_p^2}+i\alpha(t-\Delta\tau)^2\right)\right], \tag{12}$$

where τ_p and α are pulse duration and chirp parameter of the incident pulse, respectively. In order to interpret the following experimental data correctly we assume that in real experiment there is a possibility of the shift between the spectral and temporal profiles of the incident pulse. To account for this we have included into Eq. (12) the arbitrary temporal shift $\Delta\tau$ between the extremes of pulse frequency and intensity profiles. In our experiments the incident pulse has the temporal width $\tau_p=550$ fs and spectral width $\Delta\omega/\omega_0=0.01$, that corresponds to $|\alpha\tau_p^2|=12.77$.

It is well known that in the medium with quadratic frequency dispersion when the phase of transmitted wave is reasonably approximated by:

$$\phi_T=\phi_T(\omega_0)+\phi_T'(\omega_0)(\omega-\omega_0)+\phi_T''(\omega_0)(\omega-\omega_0)^2/2 \tag{13}$$

the chirped pulse is stretched or compressed depending on the ratio between the signs of chirp parameter α and phase second derivative ϕ''. In this case the intensity of the transmitted wave is

$$I_T(z=L,t)=\frac{I_0\tau_p^2|T_n(\tilde{\omega}_0)|^2}{\tau_p^2(1+\alpha\phi_T''(\tilde{\omega}_0))+(\phi_T''(\tilde{\omega}_0))^2}\times\exp\left[-\frac{(t+\phi_T'(\tilde{\omega}_0)+\Delta\tau)^2}{\tau_0^2}\right], \tag{14}$$

where $\tilde{\omega}_0=\omega_0-\alpha\Delta\tau$,

$$\tau_0=\tau_p\sqrt{(1+\alpha\phi_T''(\tilde{\omega}_0))^2+\frac{(\phi_T''(\tilde{\omega}_0))^2}{\tau_p^4}}. \tag{15}$$

On the other hand, it is seen from Fig. 3 that in the case of femtosecond incident pulse the phase ϕ_T cannot be approximated by Eq. (13) with reasonable accuracy. As a result, the effects of high order dispersion will appreciably affect on the temporal profile of transmitted and reflected waves.

IV. EXPERIMENTAL SETUP

A schematic diagram showing the experimental set-up developed at the Université du Littoral and used for the measurements is depicted in Fig. 6.

The laser system used in our experimental set-up consists of a mode-locked Ti:Sapphire laser (Coherent, Mira 900) and regenerative amplifier (Coherent, RegA 9000), both pumped by argon-laser (Coherent, Innova 420). The main parameters of RegA 9000 output radiation are the following: pulses rep-

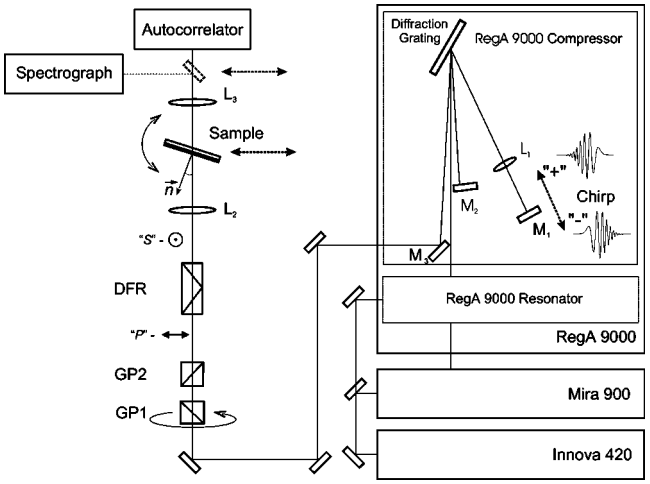

FIG. 6. Schematic diagram of the experimental used for the measurements. M_1, M_2, and L_1D1−mirrors and lens of the RegA 9000 compressor; M_3−output mirror; L_2, L_3−focusing and collimating lenses; GP1, GP2 Glan-Taylor polarizers; DFR−double Fresnel rhombus. ''*P*'' and ''*S*'' indicate state of polarization of radiation before and after DFR.

etition rate is 200 kHz with the maximal output average power as 800 mW and the central wavelength of the spectrum of the pulse is in the range of 810–820 nm; the pulse duration is $\tau_0 = 270$ fs with the spectral width $\Delta\lambda = 8$ nm (both measured at the half-maximum level). By translating the mirror M_1 in the grating compressor placed on the output of the regenerative amplifier we change the pulse duration, sign and the value of the chirp. The correspondence between the direction of M_1 translation and the sign of the chirp is schematically depicted in Fig. 6 by the arrow. The energy of the amplified femtosecond pulses was varied precisely by the Glan-Tailor prisms (GP1 and GP2). By the GP2 and the double Fresnel rhombus we set the direction of the linear polarization of the laser beam on the sample as the vertical (s-polarization). GP1 was aimed to set the energy of the pulses incoming to the PC sample on the 3.5 mW average power.

The laser beam was focused by the 8 cm lens L_2 onto the PC sample. The experimental conditions minimize any possibility of heating or PC damage. The sample is mounted on the rotary part of the goniometer in order to align and vary incident angles. The goniometers rotation axis was strictly controlled to be in the plane of the sample. The sample could be moved out of the beam path and placed back with a translation stage. Collimated with lens L3 laser beam is sent directly to autocorrelator or to spectrograph (Chromex 500IS). The spectroscopic signal detection was accomplished by a liquid nitrogen cooled CCD camera (Princeton Instruments Inc.).

In the experiments we studied both spectral and temporal properties of the radiation incoming on the PC structure and transmitted through it versus the angle of incidence θ. We measured the pulse duration (by means of second order autocorrelation function of intensity technique) and spectral profile of the pulses. The measurements of the pulse parameters were made just before and after the PC sample.

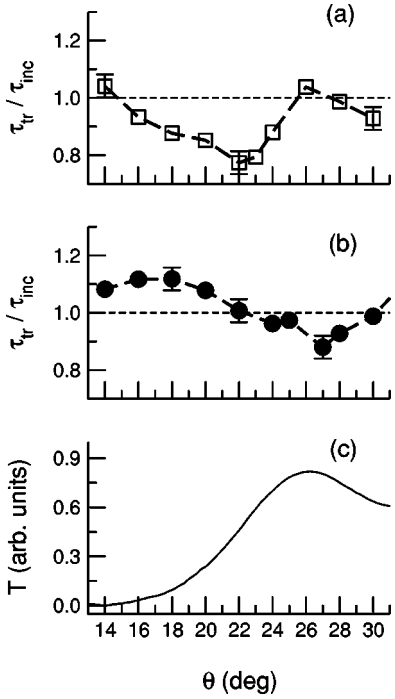

FIG. 7. Results of the measurements of relative changes of pulse duration (τ_{tr}/τ_{inc}) versus the angle of incidence θ for the pulses transmitted through the PC structure for two signs of the chirp of pulses incoming to the sample: (a) for the positive and (b) the negative ones. (c) linear transmission (T) of the structure versus the incident angle.

V. EXPERIMENTAL RESULTS

In this section we discuss and analyze our experimental results. We carried out two sets of experiments. In the first one we measured relative changes of pulse duration (τ_{tr}/τ_{inc} where τ_{tr} is the duration of the transmitted pulse and τ_{inc} is the duration of the incoming one) after its transmission trough the PC sample versus the angle of incidence θ. From the measurements of the second order autocorrelation function we extracted the FWHM of the transmitted pulses for two signs of the chirp of femtosecond pulses incoming to the sample. The typical results for the pulses with the positive sign of the chirp are indicated in Fig. 7(a) and for the negative one in Fig. 7(b). In both experimental sets the spectral width and the pulse duration of laser radiation were the same, and were measured as 8 nm and 550 fs accordingly. Both Figs. 7(a) and 7(b) show that we observe the compression of the femtosecond laser pulses that have initial nonzero value of the chirp parameter. It is clearly seen from these figures that the behavior of the pulse duration demonstrates closer tendencies for the two cases when incoming radiation obtained the chirp of opposite signs. Figure 7(a) demonstrates that if the chirp of the pulse has the positive sign, the behavior of the experimental curve has initially monotonous character. Relative pulse duration decreases with the increasing of the angle of incidence and achieves the minimum of the pulse duration at the $\theta = 22$ degrees. This particular point lies on the linear transmission band-gap edge (the linear transmission of the structure versus the incident angle is

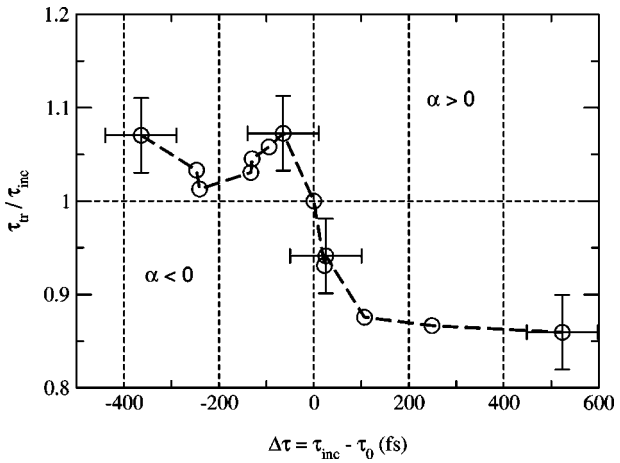

FIG. 8. Results of measurements of the relative changes of pulse duration value (τ_{tr}/τ_{inc}) versus the difference $\tau_{inc}-\tau_0$ ($\tau_0=270$ fs).

shown in Fig. 7(c) as well), where the PC sample is highly dispersive, but not strongly reflecting.

For the case of the negative sign of the chirp of the pulse, we also observed the compression, but the experimental curve does not exhibit the monotonous character. First, the relative pulse duration increases with the increasing of the angle of incidence and exhibits clear tendency for the pulse decompression with a pulse duration maximum around 18 degrees. Then, the pulse duration decreases with the minimum at 28 degrees. In fact, we observed the different pulse compression ratios for two signs of the chirp: for the positive sign, the compression is detected in two times more efficient than for the negative one.

In the second experimental set we studied the compression of the pulses in the PC structure for different values of the duration of the pulses incoming on the PC sample. The value of relative changes of pulse duration (τ_{tr}/τ_{inc}) is shown versus the difference $\tau_{inc}-\tau_0$ (here $\tau_0=270$ fs) in Fig. 8. The measurements were made for the fixed angle of incidence on the PC structure $\theta=22$ degrees and with the fixed spectral width of incoming radiation for the chirp parameter $\alpha>0$ (positive chirp) and for $\alpha<0$ (negative chirp). We observe that the pulses with the positive sign of the chirp demonstrate a reliable tendency for compression achieving the value of $\tau_{tr}/\tau_{inc}=0.85$. The pulses with the negative sign of the chirp do not demonstrate the tendency for compression for any values of the incoming pulse duration.

VI. DISCUSSION AND CONCLUSION

Figure 9 shows the variation in the intensity temporal profile of the transmitted wave for the value, $|\alpha\tau_p^2|=12.77$, and positive (a) and negative (b) signs of chirp when the angle of incidence is varied in the range $5\leqslant\theta\leqslant40$ degrees. It is seen from Fig. 9 that the most drastic variations in the shape of transmitted pulse occur in the region $20\leqslant\theta\leqslant30$ degrees, i.e., near the edge of PBG. In the case when $\Delta\tau=0$ the position of pulse peak in the quadratic dispersion medium is determined by $\phi_T'(\theta)$ and does not depend on α. Contrary

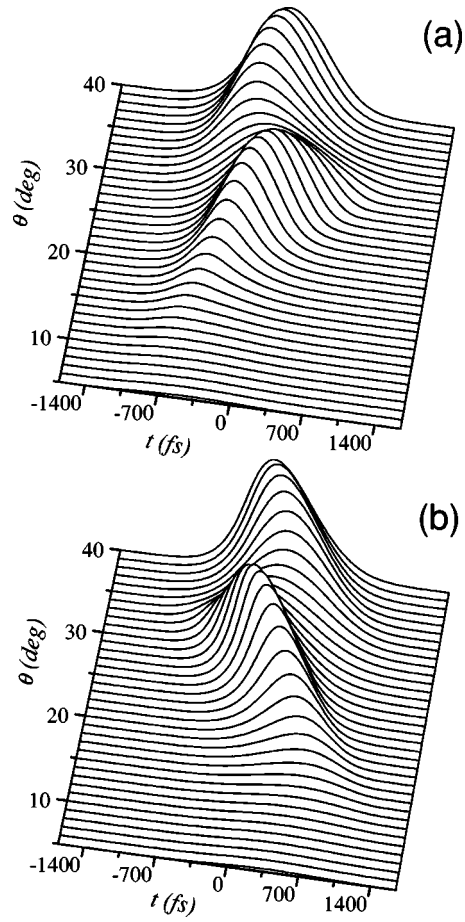

FIG. 9. Variation in the intensity temporal profile of the transmitted wave for the value $|\alpha\tau_p^2|=12.77$ for positive (a) and negative (b) signs of chirp versus incident angle.

we can see from Fig. 9 that the position of peak pulse moves with the increasing of angle of incidence in opposite directions for positive and negative sign of the incident pulse chirp. It demonstrates clearly the influence of the high-order diffraction effects on the dynamics of pulse propagation in PC. We can also see that inside PBG and far from its edge the dispersion is significantly smaller. Figure 10 shows the pulse temporal width as a function of the angle of incidence for three different values of chirp $|\alpha\tau_p^2|=8$ (a), 12.77 (b), 20 (c).

In contrast to the simple equation Eq. (15) the pulse is compressed for both signs of the chirp. The degree of compression is approximately the same for both signs but maximum of the compression is observed at different angles of incidence for two signs. The influence of temporal shift $\Delta\tau$ on the profile of the transmitted pulse is shown in Fig. 11. It is seen from Eqs. (14)–(15) and Fig. 11 that reasonable variation ($0<\Delta\tau<\tau_p$) of temporal shift $\Delta\tau$ leads to the shift along the angle of incidence axis, but it does not change the qualitative behavior of the pulse parameters as a function of angle of incidence.

The influence of the PC thickness, i.e., number of pairs of ZnS/SrF_2 layers, on the transmitted pulse profile is shown in Fig. 12. We can see that the increasing of the number of pairs of ZnS/SrF_2 layers results initially in further decreasing of

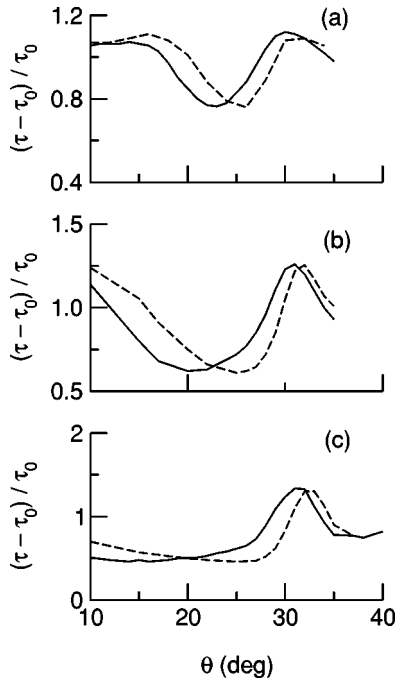

FIG. 10. Pulse temporal width as a function of incident angle for three different values of chirp $|\alpha\tau_p^2|=8$ (a), 12.77 (b), 20 (c) for positive (solid line) and negative (dotted line) signs.

pulse temporal width, but when the number of pairs exceeds nine, the pulse is broadened. This is due to two reasons. Firstly, the period of oscillations due to interference effect (see Fig. 3) is inversely proportional to the thickness of PC. As a result the width of the region where the expansion Eq. (13) holds is narrowed with the increasing of PC thickness. Secondly, and the most important, we have already mentioned that for femtosecond pulse the expansion Eq. (13) does not satisfactorily describe the dispersion of PC and the input of the high-order dispersion effects into the profile of transmitted pulse increases with the traveled distance. The

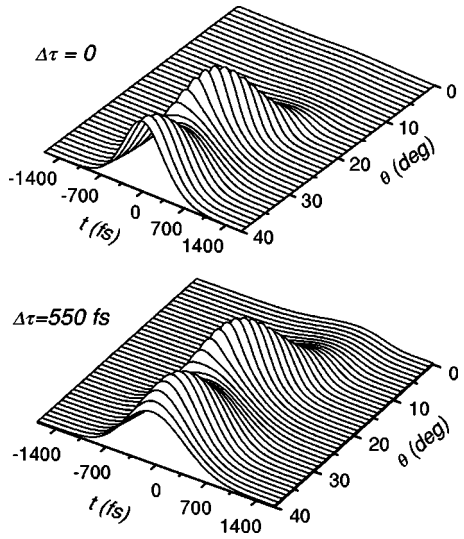

FIG. 11. Profile of the transmitted pulse for two values of temporal shift $\Delta\tau$.

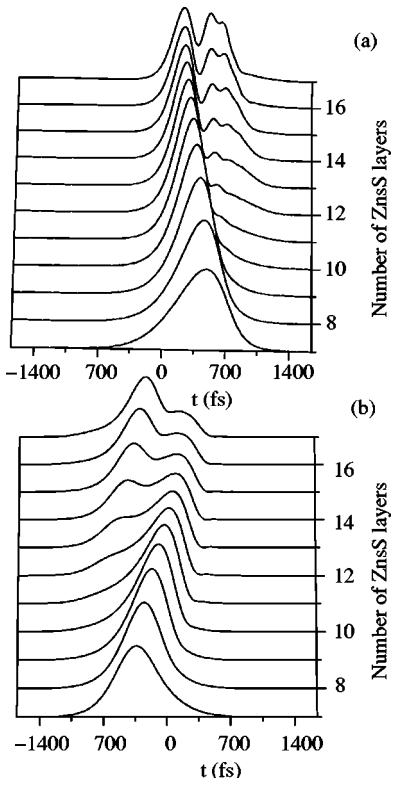

FIG. 12. Influence of the PC thickness, i.e., number of pairs of ZnS/SrF_2 layers, on the transmitted pulse profile for positive (a) and negative (b) signs of chirp.

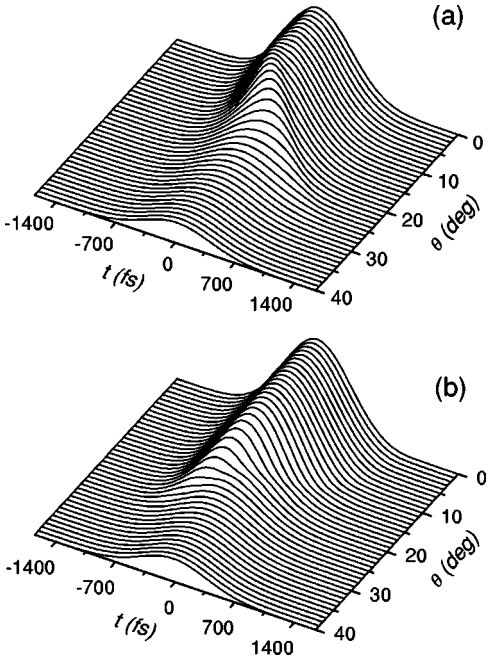

FIG. 13. Variations in the pulse temporal width and shape for reflected wave for the value $|\alpha\tau_p^2|=12.77$ for positive (a) and negative (b) signs of chirp versus incident angle.

profile of transmitted pulse becomes significantly different from that described by Eqs. (14) and (15).

The variations in the pulse temporal width and shape for reflected wave are in close analogy with that for transmitted wave and are shown in Fig. 13.

In conclusion, we have presented experimental and theoretical results of studies of compression of the femtosecond pulses in thin one-dimensional PC. We have confirmed that the experimentally observed compression of femtosecond laser pulses can be described well by the linear diffraction approach. We have also shown that the quadratic dispersion approximation Eq. (13) cannot be used for the description of the femtosecond pulse propagation in thin one-dimensional PC. This is due to the wide spectral width of this pulse. The dispersion is most important near the edge of PBG and does not significantly affect pulse propagation dynamics in thin PC when the angle of incidence is inside or far from PBG [15,28]. We would like to focus the attention on the role of this intriguing area in the phenomena concerned with the nonlinear optical frequency conversion. In the case of the femtosecond optical pulses for thin PC we may potentially observe different nonlinear optical conversion efficiencies for the pulses with different signs of the chirp. We expect to study them in more detail in the future.

ACKNOWLEDGMENTS

The authors gratefully acknowledge Dr. Yu. P. Strel'nikov for technical assistance with the sample fabrication. We would like to thank the Université du Littoral for the financial support during the course of these experiments and one of the authors (A.P. Shkurinov) is especially grateful for the support of the Région Nord/Pas de Calais. This work was supported in part by the Russian Foundation for Basic Research (Grants 99-02-16093, 98-02-17544) and BMBF (Grant 0081/99 13N7516). The Laboratoire de Physico Chimie de l'Atmosphère participates with the Centre d'Etude et de Recherche Lasers et Applications, supported by the Ministère de la Recherche, the Région Nord/Pas de Calais, and the Fond Européen de Développement Economique des Régions.

[1] L. Bragg, *Crystalline State: A General Survey* (London, Bell, 1962).
[2] C.G. Darwin, Philos. Mag. **27**, 675 (1914).
[3] E. Yablonovitch, in special issue of J. Mod. Opt. **41**, 173 (1994).
[4] *Development and Applications of Materials Exhibiting Photonic Band Gaps*, edited by C.M. Bowden, J.P. Dowling, and H.O. Everitt, special issue of J. Opt. Soc. Am. B **10**, 279 (1993).
[5] *Principles and Applications of Photonic Band Gap Structures*, edited by J.W. Haus and G. Kurizki, special issue of J. Mod. Opt. **41**, 345 (1994).
[6] A. Yariv and P. Yeh, *Optical Waves in Crystals. Propagation and Control of Laser Radiation*, (John Wiley & Sons, New York, 1984).
[7] J. D. Joannopoulos, R. D. Meade, and J. N. Winn, *Photonic Crystals: Modeling the Flow of Light* (Princeton University Press, Princeton, 1995).
[8] J.P. Dowling and C.M. Bowden, in special issue of J. Mod. Opt. **41**, 345 (1994).
[9] J.M. Bendickson, J.P. Dowling, and M. Scalora, Phys. Rev. E **53**, 4107 (1996).
[10] Y.R. Shen, *The Principles of Nonlinear Optics* (John Wiley & Sons, New York, 1984).
[11] M.J. Steel and C. Martijn de Sterke, Opt. Lett. **21**, 420 (1996).
[12] A.V. Balakin, D. Boucher, V.A. Bushuev, N.I. Koroteev, B.I. Mantsyzov, I.A. Ozheredov, A.P. Shkurinov, D. Boucher, and P. Masselin, Opt. Lett. **24**, 793 (1999).
[13] A.V. Andreev, O.A. Andreeva, A.V. Balakin, D. Boucher, P. Masselin, I.A. Ozheredov, I.R. Prudnikov, and A.P. Shkurinov, Quantum Electron. **29**, 632 (1999).
[14] A.V. Balakin, V.A. Bushuev, B.I. Mantsyzov, P. Masselin, I.A. Ozheredov, A.P. Shkurinov, and D. Boucher, JETP Lett. **70**, 725 (1999) [Pis'ma Zh. Éksp. Teor. Fiz. **70**, 718 (1999)].
[15] B.J. Eggleton, R.E. Slusher, C. Martijn de Sterke, P.A. Krug, J.E. Sipe, Phys. Rev. Lett. **76**, 1627 (1996).
[16] B.J. Eggleton, C. Martijn de Sterke, and R.E. Slusher, Opt. Lett. **21**, 1223 (1996).
[17] B.J. Eggleton, G. Lenz, R.E. Slusher, N.M. Litchinitser, Appl. Opt. **37**, 7055 (1998).
[18] B.J. Eggleton, C. Martijn de Sterke, and R.E. Slusher, J. Opt. Soc. Am. B **16**, 587 (1999).
[19] H.G. Winful, Appl. Phys. Lett. **46**, 527 (1985).
[20] A.M. Zheltikov, N.I. Koroteev, S.A. Magnitskii, A.V. Tarasishin, Quantum Electron. **28**, 861 (1998); N.I. Koroteev, S.A. Magnitskii, A.V. Tarasishin, and A.M. Zheltikov, Opt. Commun. **159**, 191 (1999).
[21] R.A. Vlasov and A.G. Smirnov, Phys. Rev. E **61**, 5808 (2000).
[22] M. Scalora, R.J. Flynn, S.B. Reinhardt, R.L. Fork, M.J. Bloemer, M.D. Tocci, C.M. Bowden, H.S. Ledbetter, J.M. Bendickson, J.P. Dowling, and R.P. Leavitt, Phys. Rev. E **54**, R1078 (1996).
[23] A.G. Smirnov, Opt. Spectrosc. **87**, 555 (1999).
[24] A.V. Andreev, A.V. Balakin, D. Boucher, I.A. Ozheredov, P. Masselin, and A.P. Shkurinov, JETP Lett. **71**, 539 (2000).
[25] F. Ouellette, Opt. Lett. **12**, 827 (1987); L. Poladian, F. Ladouceur, and P.D. Miller, J. Opt. Soc. Am. B **14**, 1339 (1997).
[26] J.E. Sipe, L. Poladian, and C. Martijn de Sterke, J. Opt. Soc. Am. A **11**, 1307 (1994).
[27] L.G. Parratt, Phys. Rev. **95**, 359 (1954).
[28] S. Wang, H. Erlig, H.R. Fetterman, E. Yablonovitch, V. Grubsky, D.S. Starodubov, and J. Feinberg, Microwave Opt. Technol. Lett. **20**, 17 (1999).